# Evidence for subglacial ponding across Taylor Glacier, Dry Valleys, Antarctica

Alun HUBBARD,[1] Wendy LAWSON,[2] Brian ANDERSON,[2] Bryn HUBBARD,[3] Heinz BLATTER[4]

[1]*Department of Geography, University of Edinburgh, Drummond Street, Edinburgh EH8 9XP, UK*
*E-mail: alh@geo.ed.ac.uk*
[2]*Department of Geography, University of Canterbury, Private Bag 4800, Christchurch, New Zealand*
[3]*Centre for Glaciology, Institute of Geography and Earth Sciences, University of Wales, Aberystwyth, Aberystwyth, Dyfed SY23 3DB, UK*
[4]*Institute of Geography, Swiss Federal Institute of Technology (ETH), CH-8057 Zürich, Switzerland*

**ABSTRACT. Ice-penetrating radar and modelling data are presented suggesting the presence of a zone of temperate ice, water ponding or saturated sediment beneath the tongue of Taylor Glacier, Dry Valleys, Antarctica. The proposed subglacial zone lies 3–6 km up-glacier of the terminus and is 400–1000 m across. The zone coincides with an extensive topographic overdeepening to 80 m below sea level. High values of residual bed reflective power across this zone compared to other regions and the margins of the glacier require a high dielectric contrast between the ice and the bed and are strongly indicative of the presence of basal water or saturated sediment. Analysis of the hydraulic equipotential surface also indicates strong convergence into this zone of subglacial water flow paths. However, thermodynamic modelling reveals that basal temperatures in this region could not exceed –7°C relative to the pressure-melting point. Such a result is at odds with the radar observations unless the subglacial water is a hypersaline brine.**

## INTRODUCTION

Thermal conditions at the beds of polar glaciers and ice sheets are important not only because they have a fundamental bearing on ice dynamics through basal sliding and sediment deformation but also because they exert a critical control on glacier erosion, sediment entrainment, transport and deposition (Sugden and John, 1976). Furthermore, investigations of large, long-lived subglacial lakes underlying the East Antarctic ice sheet (EAIS) highlight the role that ice-sheet thermomechanics plays in their extent, volume and continued longevity. Herein, we present field and modelling data that indicate the existence of a warm, wet-based zone under the tongue of Taylor Glacier, an outlet glacier of the EAIS terminating within the Dry Valleys. Robinson (1984) suggested on the basis of theoretical evidence that Taylor Glacier has extensive areas of temperate basal ice. The ice-penetrating radar and modelling evidence presented extends this interpretation and has implications for the genesis of debris-laden ice which, at Taylor Glacier, is most likely adfrozen to the sole of the glacier from an overdeepening, 5 km up-glacier of the terminus, to which it is subsequently advected and becomes exposed.

Debris-laden ice (DLI) has been observed at the base of a number of glaciers and ice caps in Arctic and Antarctic regions where the prevailing climatic regime yields a predominantly frozen (or cold) ice–bed interface (Mercer, 1971; Gemmell and others, 1986; Fitzsimons, 1996; Gow and others, 1997). The presence of DLI is important because it is less viscous than pure glacier ice at the same temperature and thus, where present, exerts an influence on ice dynamics. Holdsworth and Bull (1970) observed that the 'opaque basal ice' of Meserve Glacier, Dry Valleys, was significantly softer than debris-free ice at the same temperature (–18°C), yielding a flow-law exponent of 4.5 compared to 1.9 for the overlying glacier ice. Holdsworth and Bull (1970) tentatively associated this observed contrast in rheology with the impurities present in the basal layer at Meserve Glacier. Investigations into the genesis of such layers have generally concluded that the necessary entrainment occurs whilst the bed of the glacier is at the pressure-melting point, yielding conditions advantageous to melting and refreezing, abrasion, plucking and entrainment (e.g. Knight and others, 1994).

However, Cuffey and others (2000), in their detailed analysis of the gas and isotopic composition of Meserve Glacier, propose that the basal DLI layers observed at that site result from entrainment occurring at subfreezing temperatures. These authors invoke the presence of a supercooled interfacial water film at –17°C to refine a mechanism first proposed by Shreve (1984) by which cold-based ice slides over microscale roughness elements through regelation. Thus even under frozen bed conditions this mechanism will give rise to the processes of abrasion and striation, and the generation of erosive fines. Such an important conclusion, they note, provides a significant challenge to the widely held view that cold-based glaciers are protective of their substrates and only wet-based glaciers are capable of accomplishing any significant geomorphic work on the landscape.

The field and modelling evidence presented here that indicates temperate subglacial conditions, and possibly water ponding, across the bed of Taylor Glacier tongue is important because this glacier also has a well-developed and extensive basal DLI layer, similar to that observed at Meserve Glacier. Although this correspondence of wet-bed conditions and DLI does not discount the above hypothesis for cold-based entrainment of debris, it does indicate that the thermal character of the bed of Taylor Glacier, and

https://doi.org/10.3189/172756404781813970 Published online by Cambridge University Press

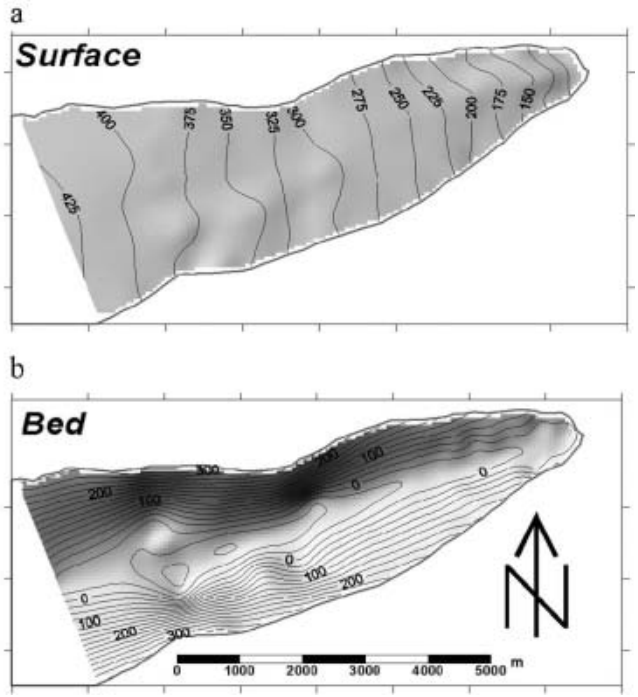


**Fig. 1.** The surface (a) and subglacial bed (b) topography of Taylor Glacier tongue interpolated onto 50 m grids from GPS, radar and ice-margin surveys. Units in m and contoured at 25 m intervals.

possibly other glaciers in the Dry Valleys, may be more complex than Cuffey and others (2000) recognized.

## FIELD AREA AND METHODS

Taylor Glacier (77°43′ S, 162°15′ E) is a 100 km long outlet of Taylor Dome, part of the EAIS, which breaches the Transantarctic Mountains and terminates at the head of one of the major valley systems of the Dry Valleys, south Victoria Land. Our study is concerned with the lower 10 km tongue of this glacier, which is 1–3 km wide and is bounded by ice cliffs, up to 35 m high, which extend some 6 km up-glacier from the terminus. With a mean annual surface temperature of –17°C at its terminus (Robinson, 1984), it is generally believed that sublimation accounts for up to 80% of the ablation over glaciers in the Dry Valleys. However, active dry-calving of the glacier's margins is also occurring, and observations in 2001/02 indicate that in exceptional summers, when ambient air temperatures exceed 0°C for extended periods, substantial amounts of supraglacial meltwater are generated which activate ephemeral fluvial channels (personal communication from T. Nylen, 2002). Debris-poor and relatively homogeneous glacier ice is underlain by a layer of DLI that is 0.5–3 m thick across the terminus of the glacier and ~3 km up both margins. This DLI merges indistinctly into the underlying frozen sediments.

### Ice-penetrating radar

The ice-penetrating radar used is based on the Narod and Clarke (1994) impulse transmitter in conjunction with an airwave-triggered Tektronix 100 MHz digital oscilloscope, a system which has been extensively used to determine basal topography, hydrological conditions and englacial structure at both temperate and polythermal glaciers (e.g. Sharp and others, 1993; Welch and others, 1998; Pattyn and others, 2003). Inline orientated (E-plane) resistivity loaded dipoles were used for the transmitter and receiver and sized for a centre frequency of 10 MHz. The scope traces were recorded digitally, along with position, using a Trimble 4700 differential global positioning system (GPS) and two base stations, which yielded a precision of <1 m in most instances. Traces and positions were recorded on foot at ~900 locations on six transects to 2 km beyond Church Rock, located ~6 km up-glacier from the terminus. The margins and terminus were also surveyed optically along with the approximate cliff angle, height and any notable glacier or basal ice facies at ~70 m intervals.

### Ice depth

Ice depth at each location was determined by manually picking the two-way travel time from each digital trace assuming a wave propagation velocity through ice of 0.17 m ns$^{-1}$. Since the digital oscilloscope was airwave-triggered, a static correction for the separation of the transmitter and receiver of 15 m was made assuming an airwave velocity of 0.3 m ns$^{-1}$. Despite generally low background scatter due to the absence of internal reflectors, yielding good bed signals in over 800 traces, 225 of the traces yielded a confused basal reflection, probably due to complex topography or basal layering. Such traces were ignored and the remaining ice-thickness measurements were estimated to be accurate to ~16%, up to 68 m in the deepest regions. In conjunction with the measured surface and margin GPS positions, these ice depths were used to produce glacier surface and bed DEMs (Fig. 1a and b) on 50 m horizontal grids using a kriging interpolation which honoured the input elevations. The resulting surface and bed DEMs have an estimated error of up to 15 and 75 m respectively. These data are used to provide topographic boundary conditions for thermomechanical modelling and to calculate the subglacial hydraulic potential ($\Phi$) surface using Shreve's (1972) relation:

$$\Phi = \rho_w g B + f \rho_i g (S - B), \quad (1)$$

where $\rho_w$ and $\rho_i$ are the densities of water and ice respectively, $g$ is gravity, $S$ is the glacier surface elevation, $B$ the bed elevation and $f$ is a factor between 0 and 1 which indicates the connectivity between the bed and atmosphere, which determines the subglacial water pressure as a fraction of the overburden pressure (Fig. 2a and b).

### Internal and bed reflection power

Following the method specified by Gades and others (2000) and further refined by Copland and Sharp (2001) for a high-Arctic glacier, the scope traces were analyzed for relative internal reflection power (IRP) and bed reflection power (BRP) to provide insight into conditions at the ice–bed interface of the glacier. This procedure was carried out simultaneously with the picking routine described above, and involved the integration of the return traces from three manually specified points along the time axis: (1) 600 ns after the surface-wave peak, (2) 200 ns before the bed-signal peak, and (3) 600 ns after the bed-signal peak. Such variable 'time windows' following the procedure of Copland and Sharp (2001) were necessary in order to capture total BRP.

Since BRP is highly dependent on the path length of the returned signal through geometric spreading, dielectric absorption and scatter from internal features, it is necessary to isolate these effects before it can be used to infer basal conditions. Following Copland and Sharp (2001), all traces

https://doi.org/10.3189/172756404781813970 Published online by Cambridge University Press

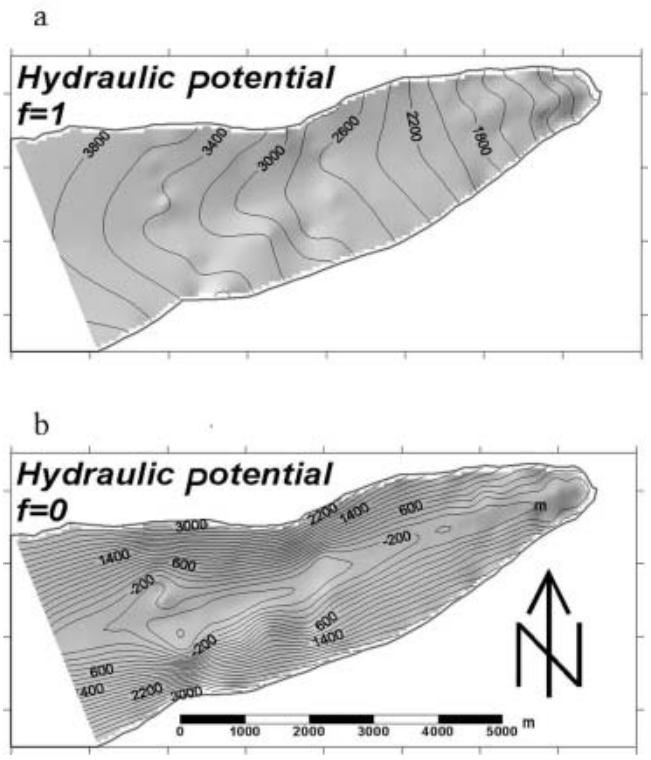


**Fig. 2.** Calculated subglacial hydraulic potential surfaces for (a) $f = 1$ where the basal hydrological system is fully isolated from the atmosphere, and (b) $f = 0$, where the basal hydrological system is completely connected to the atmosphere. Units in kPa and contoured at 200 kPa intervals.

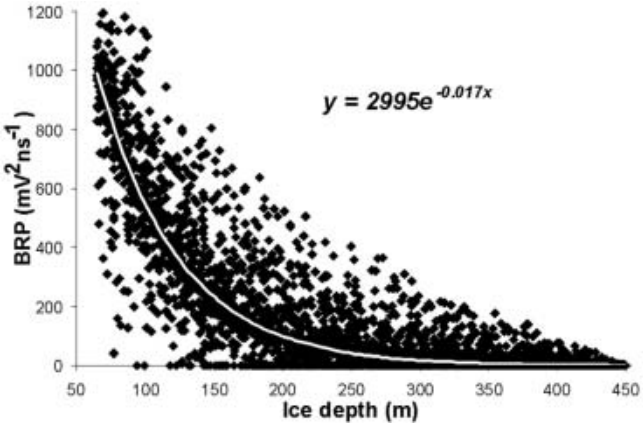


**Fig. 3.** The relationship between ice depth and bed reflection power (BRP) for the radar traces where the ratio of BRP to internal return power was suitably high. The best-fit exponential function is overlain and represents the predicted attenuation of BRP with ice depth.

that yielded large values of IRP (>2 $mV^2\,ns^{-1}$), corresponding to internal structures which could potentially absorb much of the transmitted signal, were excluded from the analysis. This left 408 traces with a high BRP/IRP ratio with which to establish an empirical relation between BRP and ice thickness to isolate the effects of geometric spreading and dielectric absorption. An exponential function with an $R^2$ of 0.80 yielded the least-squares best-fit relation between BRP and ice depth (Fig. 3). From this relation, the residual, or depth-corrected, $BRP_R$ was calculated following Gades and others (2000) by dividing the measured BRP by the predicted BRP. The resulting $BRP_R$ ratio, now corrected for depth attenuation effects, has high values in traces recording a strong basal signal, and low values in traces recording a low bed reflectivity. The technique thereby provides a means by which the distribution of $BRP_R$ may be used to infer basal conditions.

## Thermomechanical modelling

To calculate thermal conditions across the bed of Taylor Glacier tongue, a thermal model was applied based on the heat supplied to the bed by geothermal flux and friction from ice deformation, and the temperature gradient required to conduct that heat away. Frictional heating supplied to the bed ($H$) is calculated by:

$$H = -\rho_i g \nabla(S) Q_i\,, \qquad (2)$$

where $\nabla(S)$ is the ice surface slope, and $Q_i$ is the ice discharge. Under the assumption that the majority of motion, and thus heating, takes place in the lowest layers of the glacier (i.e. within the DLI), then frictional heating ($H$) and the geothermal heat flux ($G$) can be combined to yield the steady-state temperature gradient required to maintain thermal equilibrium:

$$H + G = k\frac{\partial T}{\partial z}\,, \qquad (3)$$

where $k$ is the thermal conductivity of ice and $\partial T/\partial z$ is the vertical temperature gradient. Vertical integration of this relation yields an expression for the internal and basal temperature of the glacier under an assumed surface temperature boundary condition. A value of 88.0 Mw $m^{-2}$ was taken for the geothermal heat flux ($G$) on the basis of Decker and Bucher's (1977) measurements at the base of boreholes nearby at the geologically similar Lake Vanda, during the Dry Valleys Drilling Project. The surface temperature field was determined from Robinson's (1984) temperature measurements at the base of a series of short ice-core holes into the surface of Taylor Glacier which yield a mean annual surface temperature of –17°C at the terminus and a lapse rate of 0.004 C $m^{-1}$.

The above thermal scheme was implicitly coupled with Blatter's (1995) first-order approximation and applied in three dimensions bounded by the surface and bed DEMs at 150 m resolution. The model was modified to provide a dual-layer rheological domain so as to account for the softer DLI layer in accordance with Hubbard and others (in press). By optimizing modelled flow against measured surface velocities and displacements in a vertical cliff section, Hubbard and others (in press) were able to determine values for a flow enhancement factor ($A_E$) and exponent ($n$) of 2.3 and 1 for glacier ice, and 58.0 and 4 for DLI, in Glen's generalized flow law (Nye, 1953). These values for glacier ice and DLI yield a close fit with the observed measurements and are also in accordance with the results of Holdsworth and Bull (1970) for Meserve Glacier (above).

# RESULTS AND DISCUSSION

## Topography and hydraulic potential

The main feature of the lower tongue of Taylor Glacier is the substantial overdeepening to 80 m below sea level which lies 3–6 km up-glacier from the terminus (Fig. 1b). This over-

https://doi.org/10.3189/172756404781813970 Published online by Cambridge University Press

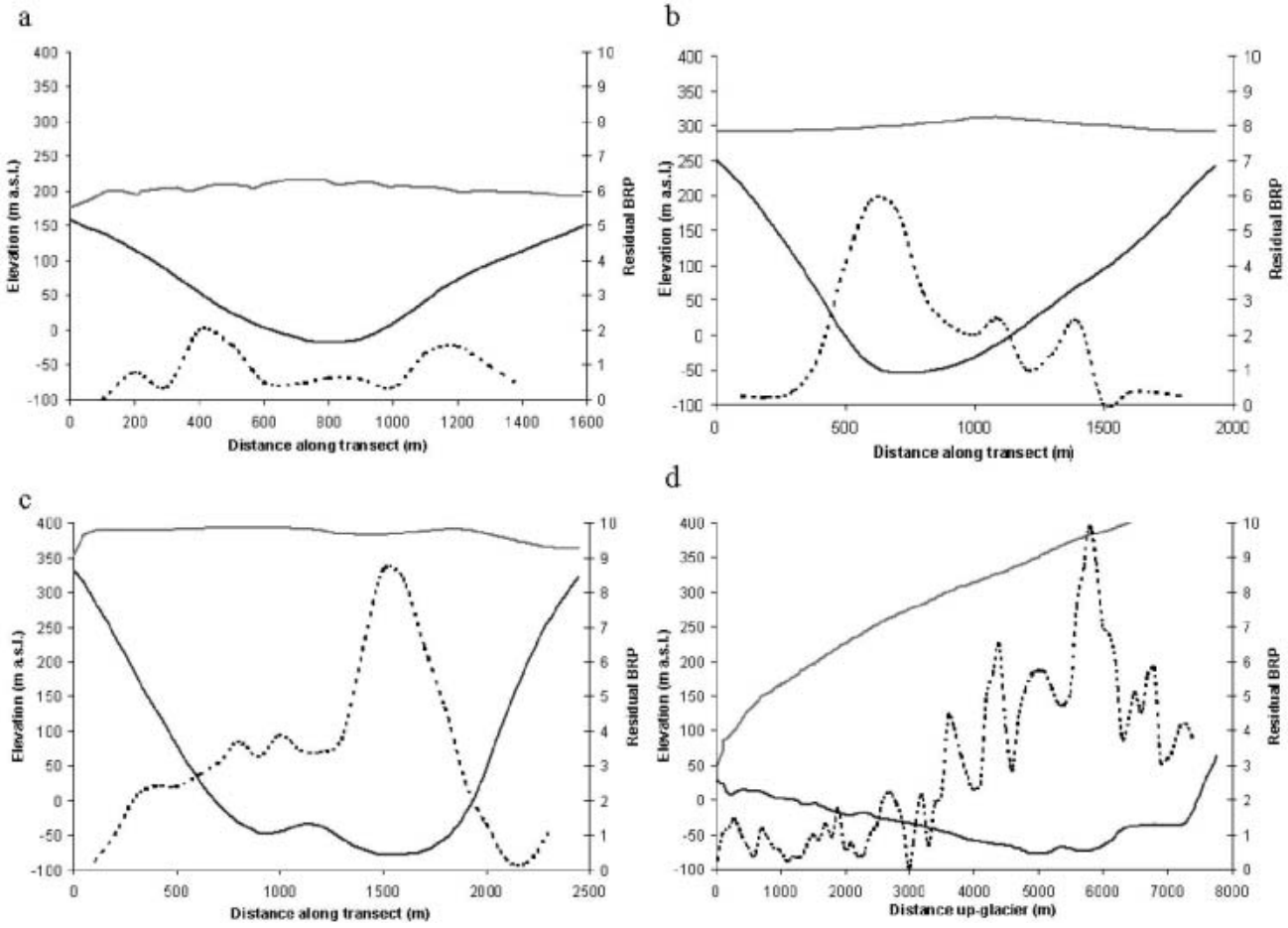


**Fig. 4.** The distribution in $BRP_R$ (dotted line) overlain on the glacier surface and bed geometry (solid lines) for three cross-profiles (a–c) and the long profile up the glacier centre line (d).

deepening corresponds to a maximum ice depth of 470 m but does not appear to influence the glacier surface markedly. Apart from a bed-induced bulge on its southern margin, this surface rises with a uniform gradient from 80 m at the terminus to 420 m ~8 km up-glacier (Fig. 1a).

The subglacial hydraulic potential surfaces with total isolation of the hydrological system from the atmosphere ($f = 1$; Fig. 2a) and complete connectivity of the hydrological system with the atmosphere ($f = 0$; Fig. 2b); both indicate strong convergence of subglacial water pathways into the overdeepening (Fig. 1b). Noting that any water present at the bed is likely to be routed from areas of high to low hydraulic potential, and normal to the equipotential contours, then the strongest convergence of basal water flow corresponds to an area ~5 km up-glacier where the bed gradient is steepest. Across the lower glacier tongue, the subglacial hydraulic equipotential indicates strong divergent routing of any basal waters away from the glacier centre line and towards the margins. The subglacial drainage reconstruction under the assumption that the hydrological system is fully connected to the atmosphere ($f = 0$; Fig. 2b) does not substantially alter the hydraulic potential surface across the upper tongue, but does indicate that under these hydraulic conditions extensive subglacial water ponding may occur within the overdeepening. In both cases, it is possible to conclude that there is a strong topographic control of subglacial water routing, if such water were present, at Taylor Glacier.

## Residual bed reflection power

The calculated distribution of $BRP_R$ across Taylor Glacier tongue displays marked spatial contrasts: predominantly low values (< 2) are recorded at the margins and along the lower tongue, and higher values of 5–8 within the central region of the upper tongue (Fig. 4a–d). The two upper cross-profiles (Fig. 4b and c) located 4 and 5.5 km up-glacier from the terminus yield maximum $BRP_R$ values of 6 and 7 respectively. These correspond closely to the lowest point of the bed topography. Subsequent values of $BRP_R$ appear to fall off rapidly towards the margins. The lowest cross-profile, located 2 km up-glacier from the terminus (Fig. 4a), has generally low $BRP_R$ but does exhibit peaks of 2 and 1.5 which occur ~400 m either side of the topographic low-point located at the middle of the transect. Although the long-profile $BRP_R$ distribution (Fig. 4d) also exhibits much heterogeneity, a more consistent trend of $BRP_R$ is observed with values increasing from generally less than 2 for some 3.5 km up-glacier, to values of consistently over 4 and up to 8 from 4.5 to 7 km up-glacier from the terminus.

Since water has a considerably higher dielectric constant than ice and rock, and the power of a reflected signal is strongly related to the dielectric contrast between the interfacing materials, it follows that a high $BRP_R$ most likely indicates wet or temperate conditions at the bed, while a low $BRP_R$ is interpreted in terms of frozen or cold basal conditions. With this assumption in mind, a strong

https://doi.org/10.3189/172756404781813970 Published online by Cambridge University Press

correspondence can be noted between both the basal overdeepening (Fig. 1b) and associated convergence of subglacial water pathways directed by the hydraulic equipotential surface (Fig. 2a and b) and the distribution of high $BRP_R$ observed across the upper tongue. Furthermore, beneath the lower glacier tongue, the $BRP_R$ maxima (Fig. 4a) displaced towards the margins correlate well with the two main subglacial pathways predicted by the subglacial hydraulic equipotential surface (Fig. 3a and b) which anticipates divergent flow away from the glacier centre line towards the margins in this region. Based on the correspondence between high $BRP_R$ and subglacial drainage indicated by the hydraulic equipotential surface, it does seem very likely that there is a real relationship between high $BRP_R$ and the presence of temperate ice, water or saturated sediments at the base of Taylor Glacier. However, despite this high level of correspondence, the association between high $BRP_R$ and the presence of water cannot be made with certainty. It is possible, for example, that the measured variations in $BRP_R$ are indicative of disparities in the basal character at Taylor Glacier, but that they denote the extent or thickness of basal DLI rather than the distribution of thermal conditions per se. Although this possibility cannot be discounted entirely, there are two arguments against it. First, the very high values ($<15$) of $BRP_R$ observed require a substantial difference in dielectric constant (d.e.) across the interface generating them. Such a dielectric contrast is only likely to be realistically obtained within a glacier between ice (d.e. $\sim 4$) and water at 0°C (d.e. $\sim 88$) (Copland and Sharp, 2001). Second, low $BRP_R$ values are measured even where distinct basal DLI layers up to 3 m thick are exposed at the margins of Taylor Glacier. In reality, it is likely that the observed variation in $BRP_R$ denotes the distribution of a combination of both thermal conditions and the extent of DLI at the bed of Taylor Glacier. That 225 radar traces returned exhibited strong, but confused, bed signals, despite little internal background noise, indicates that both the thermal conditions and structure at the bed of Taylor Glacier may be complex.

## Basal thermal conditions

The distribution of modelled basal temperature under Taylor Glacier tongue shows large variations: from –18°C at the uppermost margins to –7.8°C at the centre of the overdeepening (Fig. 5). That the highest temperature modelled at the bed coincides with the overdeepening is not unexpected since it is here that the overlying ice is at its thickest, yielding maximum insulation and frictional heating arising from glacier motion. However, nowhere across the glacier tongue do modelled temperatures approach the pressure-melting point (PMP). Sensitivity analysis of the thermally coupled first-order flow model reveals that this modelling result is robust. This is largely because Taylor Glacier tongue is currently too thin to sufficiently insulate the bed, while ice velocities ($<7\,m\,a^{-1}$ across the glacier tongue) provide little frictional heating. It is also pertinent to note that the modelled temperature distribution presented here is a liberal one, since not all the frictional heating component is likely to be delivered exclusively to the glacier bed, as is implicitly assumed in the thermally coupled flow model.

Robinson (1984) concluded that up to 50% of the bed of Taylor Glacier may be at the PMP, but this study focused on an area up-glacier of the present study where the ice was thicker. Thus, significantly less than 50% of the lower tongue

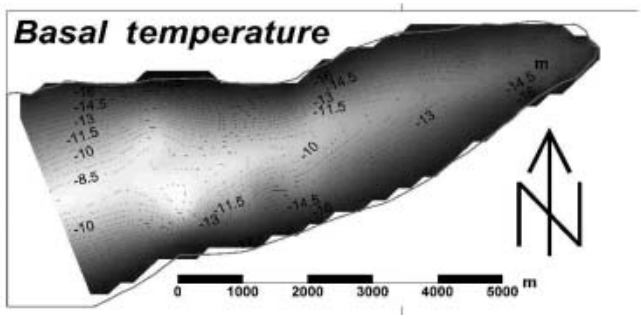


**Fig. 5.** The modelled subglacial temperature distribution under Taylor Glacier tongue. Values in °C and contoured at 0.5°C intervals.

of the glacier would be expected to be at the PMP on the basis of Robinson's analyses. This inference is consistent with the thermal modelling presented above. Hence, Robinson's and our results indicate that the base of the lower tongue of Taylor Glacier is well below the PMP. This interpretation is at odds with our $BRP_R$ analysis, though, which suggests that an extensive zone of water is present in some form at the glacier bed. A possible reconciliation of these apparently contradictory results may be provided by Doran and others (2003), who reported the presence of hypersaline brine at the base of nearby Lake Vida. Until recently, Lake Vida was presumed to be solid and frozen to its bed, but a 16 m core revealed that the permanent ice cover is underlain by water with salinity up to seven times that of sea water, allowing it to remain liquid below –10°C (Doran and others, 2003). The chemistry of Blood Falls, a deep-orange-coloured ice feature emerging from the terminus of Taylor Glacier, which contains high concentrations of both iron oxide and salt thought to have a marine origin (personal communication from H. Keys, 1999), lends support to the hypothesis that the glacier bed could indeed be hypersaline.

## CONCLUSIONS

The high correlation between the pattern of high $BRP_R$ and the predicted locations of subglacial water pathways indicates that there is water present under Taylor Glacier tongue. The relationship between $BRP_R$ and the presence of wet conditions is most likely since the dielectric constant of water is significantly higher than that of any other naturally occurring subglacial material whose presence could reasonably be expected. However, the actual hydraulic conditions present are undefined and could take any form, from a thin distributed water film to extensive water ponding or even a thick layer of saturated sediments. It can be noted, though, that 225 of the radar traces exhibited a correspondence of wet-bed conditions with a complex basal structure as would be anticipated from the presence of an extensive layer of DLI. The presence of liquid water at the bed of Taylor Glacier can only be reconciled with thermal modelling, which indicates basal temperatures of lower than –8°C, if that water is hypersaline. Such an interpretation is consistent with the presence of salt-rich ice at the glacier. The interpretation may also have bearing on investigations of sediment entrainment and transport of DLI that have hitherto reasonably assumed the presence of a frozen basal interface at sub-zero temperatures.

https://doi.org/10.3189/172756404781813970 Published online by Cambridge University Press

## ACKNOWLEDGEMENTS

We are indebted to Antarctica New Zealand and the University of Canterbury for logistical support, and to R. Hindmarsh for assistance with the fieldwork. A.H. gratefully acknowledges support from the Royal Society of Edinburgh, the Royal Society of London and the Royal Geographical Society.

## REFERENCES

Blatter, H. 1995. Velocity and stress fields in grounded glaciers: a simple algorithm for including deviatoric stress gradients. *J. Glaciol.,* **41**(138), 333–344.

Copland, L. and M. Sharp. 2001. Mapping thermal and hydrological conditions beneath a polythermal glacier with radio-echo sounding. *J. Glaciol.,* **47**(157), 232–242.

Cuffey, K. M. *and 8 others*. 2000. Entrainment at cold glacier beds. *Geology,* **28**(4), 351–354.

Decker, E. R. and G. J. Bucher. 1977. Geothermal studies in Antarctica. *Antarct. J. US,* **12**(4), 102–104.

Doran, P. T., C. H. Fritsen, C. P. McKay, J. C. Priscu and E. E. Adams. 2003. Formation and character of an ancient 19-m ice cover and underlying trapped brine in an 'ice-sealed' East Antarctic lake. *Proc. Natl. Acad. Sci. USA,* **100**(1), 26–31.

Fitzsimons, S. J. 1996. Formation of thrust-block moraines at the margins of dry-based glaciers, south Victoria Land, Antarctica. *Ann. Glaciol.,* **22**, 68–74.

Gades, A. M., C. F. Raymond, H. Conway and R. W. Jacobel. 2000. Bed properties of Siple Dome and adjacent ice streams, West Antarctica, inferred from radio-echo sounding measurements. *J. Glaciol.,* **46**(152), 88–94.

Gemmell, A. M. D., M. J. Sharp and D. E. Sugden. 1986. Debris from the basal ice of the Agassiz Ice Cap, Ellesmere Island, Arctic Canada. *Earth Surf. Processes Landforms,* **11**(2), 123–130.

Gow, A. J. *and 6 others*. 1997. Physical and structural properties of the Greenland Ice Sheet Project 2 ice cores: a review. *J. Geophys. Res.,* **102**(C12), 26,559–26,575.

Holdsworth, G. and C. Bull. 1970. The flow of cold ice: investigations on Meserve Glacier, Antarctic. *International Association of Scientific Hydrology Publication* 86 (Symposium at Hanover 1968 – *Antarctic Glaciological Exploration (ISAGE)*), 204–216.

Hubbard, B., A. Hubbard, W. Lawson and B. Andreson. In press. Relative softness of clean glacier ice and debris-rich basal ice: measurement and modelling at Taylor Glacier, Antarctica. *Geophys. Res. Lett.*

Knight, P. G., D. E. Sugden and C. D. Minty. 1994. Ice flow around large obstacles as indicated by basal ice exposed at the margin of the Greenland ice sheet. *J. Glaciol.,* **40**(135), 359–367.

Mercer, J. H. 1971. Correspondence. Cold glaciers in the central Transantarctic Mountains, Antarctica: dry ablation areas and subglacial erosion. *J. Glaciol.,* **10**(59), 319–321.

Narod, B. B. and G. K. C. Clarke. 1994. Miniature high-power impulse transmitter for radio-echo sounding. *J. Glaciol.,* **40**(134), 190–194.

Nye, J. F. 1953. The flow law of ice from measurements in glacier tunnels, laboratory experiments and the Jungfraufirn borehole experiment. *Proc. R. Soc. London, Ser. A,* **219**(1139), 477–489.

Pattyn, F. *and 6 others*. 2003. Ice dynamics and basal properties of Sofiyskiy glacier, Altai mountains, Russia, based on DGPS and radio-echo sounding surveys. *Ann. Glaciol.,* **37**, 286–292.

Robinson, P. H. 1984. Ice dynamics and thermal regime of Taylor Glacier, South Victoria Land, Anatarctica. *J. Glaciol.,* **30**(105), 153–160.

Sharp, M. *and 6 others*. 1993. Geometry, bed topography and drainage system structure of the Haut Glacier d'Arolla, Switzerland. *Earth Surf. Processes Landforms,* **18**(6), 557–571.

Shreve, R. L. 1972. Movement of water in glaciers. *J. Glaciol.,* **11**(62), 205–214.

Shreve, R. L. 1984. Glacier sliding at subfreezing temperatures. *J. Glaciol.,* **30**(106), 341–347.

Sugden, D. E. and B. S. John. 1976. *Glaciers and landscape; a geomorphological approach.* London, Edward Arnold.

Welch, B. C., W. T. Pfeffer, J. T. Harper and N. F. Humphrey. 1998. Mapping subglacial surfaces of temperate valley glaciers by two-pass migration of a radio-echo sounding survey. *J. Glaciol.,* **44**(146), 164–170.